Research Article

Kun Li and Gang Zhao*

Reverse localization on composite laminates using attenuated strain wave

https://doi.org/10.1515/secm-2020-0034
Received Jul 01, 2020; accepted Sep 02, 2020

Abstract: Carbon Fiber Reinforced Polymer (CFRP) composite materials have been widely used in high-tech fields because of their outstanding physical properties. However, barely visible impact damage can be introduced by low velocity impact, which might bring tremendous risk. Monitoring impact forces is essential for the integrity and reliability of CFRP structures. In this paper, a reverse localization scheme on CFRP composite materials is developed. The scheme is based on a predictive mode of attenuated strain wave. The signals induced by low velocity impact are obtained by strain gauges. The proposed localization scheme has been verified by experimental tests of the CFRP plates with symmetrical stacking $[0/45/90/-45]_{2s}$ The errors occurring in the test can be accepted for engineering application. The calculated impact locations are generally in consistent with the testing impact locations.

Keywords: Structural Health Monitoring, CFRP composite, Strain wave, Impact localization, Reverse localization

1 Introduction

The technology of Structural Health Monitoring(SHM) can improve the safety of high-performance structures reliably, efficiently and economically, and reduce the maintenance cost of structures. Especially in the composite structure, the structure health monitoring technology is particularly important. Composite materials have been widely used in various fields for their excellent physical properties, such as automotive, aviation, aerospace, shipping and other projects. However, the brittleness of the composite resin matrix and the reinforcing fibers make the composite structure very sensitive to the impact load. In the process of using and maintaining, composite structures often encounter low velocity impact from external objects. The strain rate induced by low velocity impact is pretty low, so it will cause the Barely Visible Impact Damage (BVID) [1]. Low velocity impacts on composite structure, that will lead to structural damage and a decline in bearing capacity [2, 3], has attracted more and more attention.

In recent years, some researchers have studied the method of low velocity impact localization of composite structures, and some meaningful methods have been put forward. In general, the majority agrees with the method based on time difference. The key problem of the time difference localization method is to solve the time difference between wave propagation and wave velocity. In the previous research literature, the methods of solving wave velocity mainly included Mindlin plate theory [4] and the Raleigh-Lamb frequency characteristic equation [5], and some researchers measured wave propagation velocity by experiment. In order to get the time difference of wave propagation, many methods of signal processing are adopted, such as DB wavelet [6], Morlet wavelet [4] and so on. However, as far as composite structures are concerned,because of the influence of strain wave's reflection, refraction, scattering and noise in the propagation process, it is very hard to determine the wave velocity and the time of arrival accurately. Therefore, some researchers have studied the damage location problem of composite laminates by pure data driven method [7, 8]. That is, the statistical and data analysis method is applied to collect useful information from the collected signals. A cross correlation statistical analysis method was used to detect the delamination damage and its location. The method of multivariate data analysis, such as principal component analysis was used to detect the delamination of composite structure.

When the wave is propagating, some energy of the wave is absorbed by the medium, so the velocity and intensity of the wave propagation will gradually weaken until it completely disappears. The problem of the correlation of the displacement or energy related to the single prop-

***Corresponding Author: Gang Zhao:** Key Laboratory of Nondestructive Testing (Nanchang Hangkong University) Ministry of Education, Nanchang 330063, China; School of Mathematics and Information Sciences, Nanchang Hangkong University, Nanchang 330063, China; Email: zhaogang0209@163.com
Kun Li: School of Mathematics and Information Sciences, Nanchang Hangkong University, Nanchang 330063, China

agation mode is a hot issue in the nondestructive evaluation. The line frequency modulation wavelet transform was used to analyze the attenuation mechanism of Lamb wave [9], and then determine that Chirplet Transform (CT) can be used for Non Destructive Testing (NDT).

Matrix material, fiber material, fiber length, curing temperature and laminate structure are all the main factors that affect the energy dissipation properties of the materials. A technique for identifying the location of a delamination in a composite materials structure using the S_0 mode1 was proposed [10], and the attenuation factor of carbon fiber reinforced composite was determined by matching the amplitudes to the experimental data in a numerical model. The most common viscous damping description is the Rayleigh damping model, in which the linear combination of the mass and stiffness matrices is used. The equation (1) was defined as Rayleigh damping [11].

$$[C] = \alpha[M] + \beta[K] \tag{1}$$

where α and β are the mass and stiffness ratio coefficient, respectively. Some researchers had investigated the damping properties of fiber reinforced composites. It was found that composite materials usually exhibit higher damping capacity than metal materials [12]. The prediction model of lamb wave propagation attenuation in carbon fiber reinforced polymer has been established by model of Rayleigh damping. The attenuation of Lamb in anisotropic materials has been proved by means of both finite element method and experimental method by Bartoli *et al.* [13].

For the sake of obtaining useful information, the researchers have used a variety of sensors in the study of impact damage location. In order to acquire acoustic signals, piezoelectric ceramic sensors (PZT), PVDF piezoelectric sensors, accelerometers, acoustic emission, magnetic sensors, laser interferometer and laser Doppler velocimeter have been applied to experimental research.

Aiming at the low velocity impact localization of carbon fiber reinforced composite structure, a new method of localization is proposed based on the previous research in this paper. The dynamic strain signal induced by low velocity impact is obtained by the strain gauges. The strain wave attenuation model is established by the impact signals obtained from different impact positions. Then the reverse impact positioning is realized on the basis of the model. The CFRP laminates are used to verify the model and localization method. The strain gauges are attached to the surface of the specimen. This paper contains the following five parts. The second section introduces the working principle of the attenuation model and the localization method. The experimental equipment and sample making are introduced in the third section. The fourth section is the result and discussion of the experiment. The feasibility of the proposed method is verified by the impact of the specimen. In the fifth section, some conclusions are reported.

2 Theoretical

In this section, the principle of wavelet transform,the attenuation model and the localization method proposed in this paper are introduced.

2.1 Background of Wavelet transform analysis

The continuous wavelt transform(CWT), $W_f(a, b)$, is obtained by convolving the signal *f(t)* with the translations (a), and dilations(s) of the mother wavelt [14, 15]:

$$W_f(a, b) = a^{-\frac{1}{2}} \int_{-\infty}^{+\infty} f(t)\psi^{\star}_{a,b}\left(\frac{t-b}{a}\right) dt \tag{2}$$

where

$$\psi^{\star}_{a,b} = a^{-\frac{1}{2}}\psi\left(\frac{t-b}{a}\right) \tag{3}$$

is the Kernel function in the CWT. It is generated by shifting and scaling a mother wavelt $\psi(t)$. Moreover, the superscript * denotes a complex conjugation, $a > 0$ is a scaling factor, b is a shifting factor and $a^{-1/2}$ can ensure the integral energy given by a wavelet is independent of the dilation a.

The scaling is a primary characteristic of the wavelet analysis. The scale parameter a is the scale variable in the WT similar to a frequency variable in the Fourier transform. $\omega = \omega_0/a$ is a relational expression between frequency ω and scale parameter a, ω_0 being the central frequency of the mother wavelet. The window function both in window size frequency and time domains is $\psi(t)_{a,b}$ we can vary the window size by varying the scaling factor a to get the appropriate resolution. The primary characteristics of the wavelet analysis are multiresolution and scaling.

The constraint condition of the fuction $\psi(t)$ is given by the following equation:

$$\int_{-\infty}^{+\infty} |\psi(t)|dt < \infty \tag{4}$$

$$f(t) = \frac{1}{C_\psi}\int_{-\infty}^{+\infty}\int_{-\infty}^{+\infty}\frac{1}{a^2}W_f(a, b)\psi\left(\frac{t-b}{a}\right)dadb \tag{5}$$

where $C_\psi = \int_R \frac{|\hat{\psi}(\omega)|^2}{|\omega|} d\omega$, $\hat{\psi}(\omega)$ is the Fourier transform of $\psi(t)$.

CWT has five important properties, which are the linearity, telescopic co degeneration, shift invariance, self similarity and redundancy. DbN is abbreviated of Daubechies wavelet function, which is used in this paper. The DbN has some advantages, such as higher smoothness of the vanishing moment, better regularity, stronger frequency domain localization ability as well as better band results. The support domain of wavelet and scale function is 2N-1, and the vanishing moment is n. Except n = 1, DbN has no symmetry and explicit expression, but the square modulus of the transformation function h has an explicit expression, which is described as follows.

The $P(y) = \sum_{k=0}^{N-1} C_k^{N-1+k} y^k$, which C_k^{N-1+k} is the binomial coefficient, then

$$|m_0(\omega)|^2 = \left(\cos^2 \frac{\omega}{2}\right)^N P\left(\sin^2 \frac{\omega}{2}\right)$$

where $m_0(\omega) = \frac{1}{\sqrt{2}} \sum_{k=0}^{2N-1} h_k e^{-jk\omega}$.

2.2 Attenuation model and location algorithm

According to the elastic wave theory, there are only two forms of propagation of strain waves in the plate structure for isotropic materials, namely, shear wave and longitudinal wave. The two waves are not coupled in the propagation process and propagated at their own velocity. In thin plate medium, the wave induced by impact is propagated to the upper and lower interface of the thin plate. Because of the reflection of the wave, the wave will change and the propagation path will change. Therefore, the waves in different modes are mixed and propagate together to form a coupled wave. It is known from the previous research literature that the coupled wave has a wave equation [5].

$$\begin{cases} u_{tt} - c_1^2 \Delta u = \alpha(v-u) + \beta(v_t - u_t), in\Omega \times (0,\infty) \\ v_{tt} - c_2^2 \Delta u = \alpha(v-u) + \beta(u_t - v_t), in\Omega \times (0,\infty) \\ u(x,0) = u_0(x) \in H^1(\Omega_u), u_t(x,0) \\ = u_1(x) \in L^2(\Omega_u) \\ v(x,0) = v_0(x) \in H^1(\Omega_u), v_t(x,0) \\ = v_1(x) \in L^2(\Omega_v) \end{cases} \tag{6}$$

where c_1 and c_2 are wave propagation speed, α and β are positive, Ω_u and Ω_v are open sets in R., respectively. The vector field $r(x) = [r_1(x), \cdots, r_n(x)] \in C^2(\overline{\Omega_u} \cup \overline{\Omega_v})$ is satisfied with the following boundary conditions:

$$\begin{cases} \Gamma_1^u = \{x \in \Gamma^u : r(x) \cdot v(x) > 0\}, \\ \Gamma_0^u = \{x \in \Gamma^u : r(x) \cdot v(x) \le 0\}, \\ \Gamma_1^v = \{x \in \Gamma^u : r(x) \cdot v(x) > 0\}, \\ \Gamma_0^v = \{x \in \Gamma^u : r(x) \cdot v(x) \le 0\}, \end{cases} \tag{7}$$

$V(x)$ is an unit outer normal vector, and $x \in \Gamma_i$ the boundary condition at $i = 0, 1$ is as follows

$$\begin{cases} u(x,t) = 0, in\Gamma_0^u \times (0,\infty), \\ c_1^2 \frac{\partial u}{\partial v} = -\beta_1(x)(r \cdot v)u_t, in\Gamma_1^u \times (0,\infty), \\ v(x,t) = 0, in\Gamma_0^v \times (0,\infty), \\ c_2^2 \frac{\partial u}{\partial v} = -\beta_2(x)(r \cdot v)v_t, in\Gamma_1^v \times (0,\infty), \end{cases} \tag{8}$$

where Γ_0^u, Γ_0^v, Γ_1^u, Γ_1^v are not empty with respect to $\Gamma_i (i = 0, 1)$, $x \in R^n$ is the spatial and temporal variable, u and v are the displacement of the position, $\beta_i (i = 1, 2)$ is a boundary parameter, respectively.

The following equation can be obtained by combining equations (6) and (7)

$$\frac{dE}{dt} = \dot{E(t)} = -\beta \int_\Omega (u_t - v_t)^2 dx + \int_{\Gamma_1^u} -\beta_1 (r \cdot v) u_t^2 d\Gamma + \int_{\Gamma_1^v} -\beta_2 (r \cdot v) v_t^2 d\Gamma \le 0 \tag{9}$$

It is known that energy attenuates with time from the equation (9). The coupled wave equation (6) has exponential stability for the compressed semigroup under the boundary conditions (7) and (8). That is, there is a normal number of ω, C makes

$$E(t) \le Ce^{-\omega t} E(0) \tag{10}$$

In the process of wave propagation, due to a part of the wave energy is absorted by medium, the mechanical energy of the wave decreases and the wave intensity is gradually weakened. From the literature [16, 17], it is known that the relation between the amplitude attenuation of wave and Propagation distance of wave is given by the following equation:

$$A = Be^{-\alpha x} \tag{11}$$

B and A are the amplitudes at x=0 and x=x respectively. α is the absorption coefficient of the medium. There is a one-to-one correspondence between the amplitude of sensor induction and the position of the plate impact source. Therefore, the position of the impact source can be obtained by the following equation.

$$x = -\frac{1}{\alpha} \ln \frac{A}{B} \tag{12}$$

3 Experimental studies

In this paper, the method proposed in Section 2.2 will be verified by the experiments. The absorption coefficient of the composite plate used in this experiment is the same. The strain gauges are pasted on the templates. According to the previous literature, the paste mode can effectively detect the strain signal induced by low velocity impact.

3.1 Preparation of specimens

The CFRP templates are cured in autoclave moulding with prepreg in this experiments,as can be seen in Figure 1. The model of carbon fiber unidirectional prepreg is hrc1-30% - a12-u-150gsm, which is manufactured by Jiangsu Hengshen Co., Ltd. Physical properties of a unidirectional carbon fiber reinforced polymer material are shown in Table 1. The templates are sealed with a vacuum bag. Firstly, they are vacuumed. Then they are put into the autoclave and are cured with reference to setting program. The autoclave temperature increased from room temperature to 80°C at a rate of 2°C/min, heat preserved for 30 minutes, then kept on increasing to 120 degrees at 2°C/min, heat preserved for 90 minutes, finally reduced to 50°C at a rate of 1°C/min. The sample is removed from the autoclave after cooling. The template possesses a stacking sequence of $[0/45/90/-45]_{2s}$, its size is 450mm × 450mm × 2mm. The sample is cut into 418mm × 418mm × 2mm.

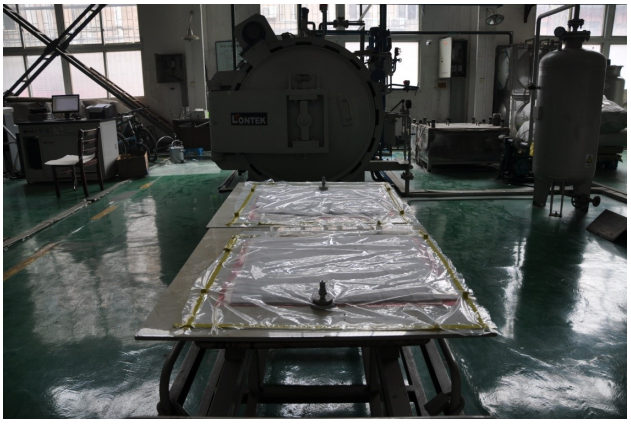

Figure 1: An illustration of sample making

Table 1: Properties of unidirectional CFRP Lamina

Property	CFRP
Longitudinal Young's modulus, E_{11} (GPa)	121
Transverse Young's modulus, E_{22} (GPa)	8.6
Longitudinal shear modulus, G_{12} (GPa)	5.9
Transverse shear modulus, G_{23} (GPa)	4.3
Poisson's ratio, v_{12}	0.31
Ply thickness(mm)	0.125
Desity, ρ (kg/m^3)	1520

The four edges of the plate are clamped tightly by M6 type bolts to fix the testing plate on the metal frame for each testing template. The geometry of the testing plate is schematically shown in Figure 2.

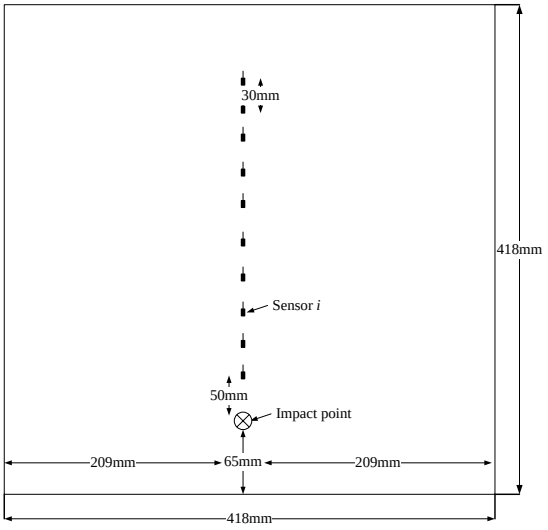

Figure 2: Sample plate size and strain gauges layout

Resistance strain gauges are used to detect and collect the wave propagation and deformation data initiated by the low energy impact. Strain gauges are simple and cheap devices that have been historically used in numerous applications for frequency response. Recently dynamic strain gauges are developed with high frequency response and are suitable for the utilization for impact localization. The strain gauge with its base of 3mm × 2.5mm is selected in this paper. The resistance of the strain gauge used in the experiment is 120Ω. As shown from Figure 2, in order to reduce the influence of boundary factors on the impact results, 10 strain gauges are pasted in the middle of the template in sequence.The distance between impact position and the first strain gauge is 50mm. The distance between the other 9 strain gages is 30mm.

3.2 Experimental instrument

The impact test of the sample includes two parts: the impact devices and the data acquisition devices .The impact device is illustrated in Figure 3. The impact device consists

Figure 3: Impact test devices and the data acquisition devices

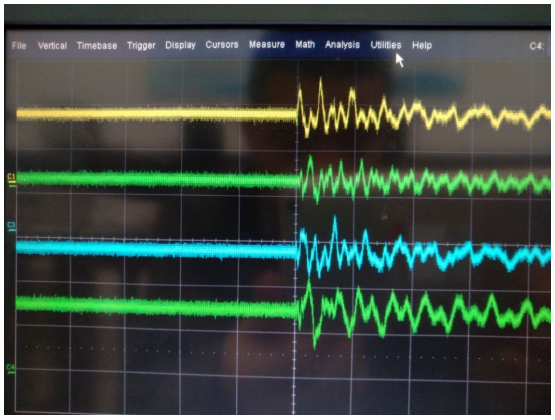

Figure 4: Waveforms of signals collected by strain gauges

of an air gun, a velometer, a clamp and a baffle. The steel bullet is long 59mm with a weight of 12.9g and a diameter of 6mm. The velometer is responsible for measuring the speed of a bullet shooting. The distance between the sample plate and the gas gun is 0.5m. The impact position distance is at the boundary 65mm. Data acquisition device are consisted of a LeCroy WaveRunner 6100A oscilloscope(Teledyne LeCroy) and a SDY2107 ultra dynamic strain meter signal amplifier (Electronic Technology Co., Ltd.) (see Figure 3). The sampling frequency is 10MHz.

4 Results and discussion

When the impact occurred, due to the damping and dispersion characteristics of CFRP, the signal will decay rapidly until all disappear, and the whole process will continue for a short time. For example, Figure 4 is the impact signal waveform acquired by the strain gauges.

From Figure 4, it can be seen that the central wavelength of the sensor is fluctuated, and the duration of the whole fluctuation is rapid. It is shown that the structure is excited by the instantaneous excitation. The maximum amplitude does not appear on the first wave peak, which indicates that after the impact of the sample plate, many synthetic waves are formed, and the synthetic waves are mixed by shear waves and longitudinal waves. When the amplitude of the signal reaches the maximum, the amplitude of the signal gradually decreases until it is completely attenuated.

In order to verify the stability of the signal induced by impact, two impacts are carried out, and the same group of strain gages is used to collect the signal. As shown in Figure 5, the signals of the two shock acquisition are basically the same

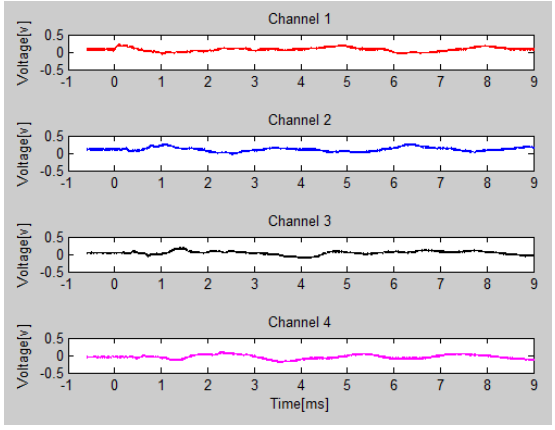

(a) The first impact

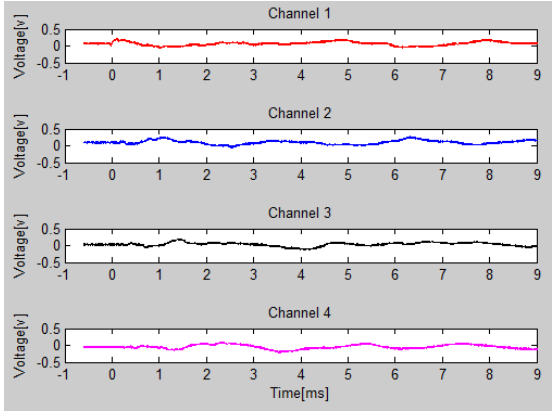

(b) The second impact

Figure 5: Example of original signals obtained from the impact tests

4.1 Extraction of amplitude

At the same speed, the impact point in Figure 2 is impacted, and the impact speed is 8.6m/s. The signal gathered from the first strain gauge is the trigger signal. The signals obtained from strain gauge No. 2-10 are collected. According

Table 2: Distance from the impact point and amplitude for the template

	1#	2#	3#	4#	5#	6#	7#	8#	9#
Distance (cm)	8	11	14	17	20	23	26	29	32
Amplitude (pm)	43.74	35	21.9	18.16	14.53	12.07	10.03	5.4	5.19

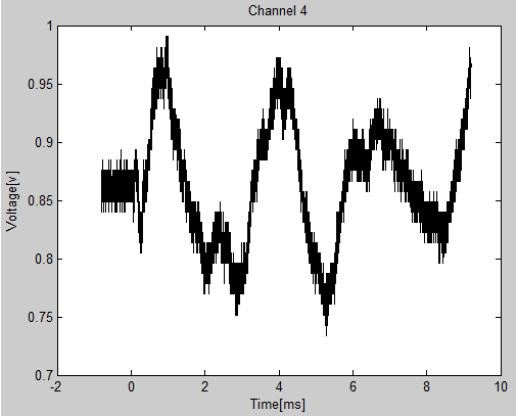

(a) Signal original diagram

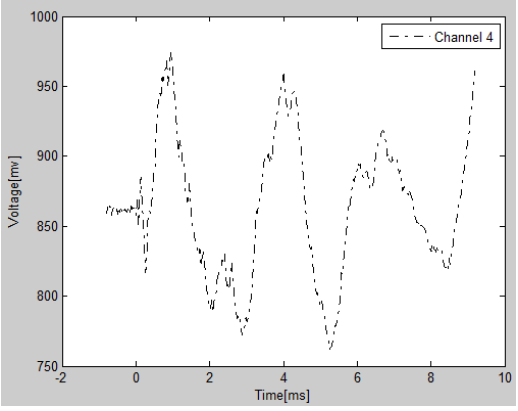

(b) Wavelet transform graph

Figure 6: Signal original diagram and Wavelet transform graph

to the 2.1 section, the Db wavelet is changed to analyse those signals. As shown in Figure 6, the original signal collected by a strain gage, then it is denoised, decomposed and reconstructed by DB wavelet.

Since the impact occurs, a lot of synthetic waves are formed due to the occurrence of damping and frequency dispersion. In order to avoid the effect of synthetic waves on the results, the first wave peak amplitude of each signal is extracted. The calculation of wave amplitude is based on the amplitude minus datum value. The signals obtained from strain gauge No. 2-10 are calculated respectively, and the results are shown in Table 2.

4.2 Result

Data from Table 2 are fitted respectively. Results of the least-squares cure-fitting method are shown in Figure 7.

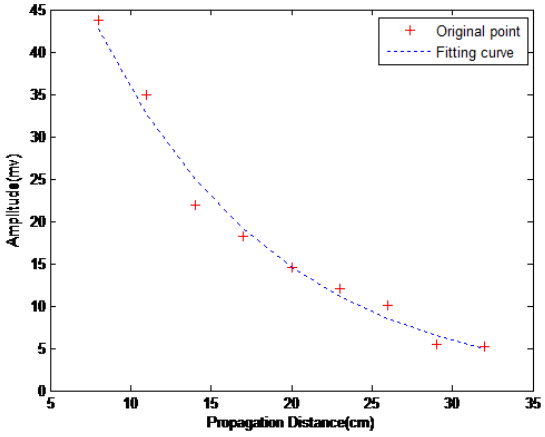

Figure 7: Fitting curve for the specimen

The calculated B and α coefficient of the specimen are 87.3397 and 0.0895, respectively.

$$ER = |((R - F)/F) * 100| \text{ is an error ratio.}$$

where R is the actual distance value, F is the fitting value. A rectangular coordinate system is established based on the origin of the impact point coordinates. According to the location algorithm proposed in 2.2 section, we choose five impact points to verify the algorithm for the specimen. The results are shown in Table 3.

The mean value of the error ratio from Table 3 is 8.77. Let P_0 (x_0, y_0) be a point calculated by the attenuation

Table 3: Validation results

No.	coordinate (cm)	Real value (cm)	Fitting value (cm)	Error (cm)	ER
1	(0, 5)	5	4.54	0.46	10.06
2	(8,0)	8	8.59	0.59	6.91
3	(−14,0)	14	12.47	1.53	12.31
4	(−8.49,8.48)	12	12.36	0.36	2.911
5	(−12.73,12.73)	18	16.12	1.88	11.64

curve on the template, the δ is a positive number. U (P_0, δ) denotes the δ neighborhood of point P_0. As shown in equation 13.

$$U(P_0, \delta) = \{P||PP_0| < \delta\} \tag{13}$$

where $\delta = F \times (1 + 8.77\%)$.

It is known from the Table 3 that the confidence level of the impact source falling in the neighborhood U (P_0, δ) is 0.98.

4.3 Discussion

After the impact, the sample was scanned by C scan. As shown in Figure 8, no damage was found in the impact position. It shows that many tests conducted at the same location did not affect the experimental results due to damage.

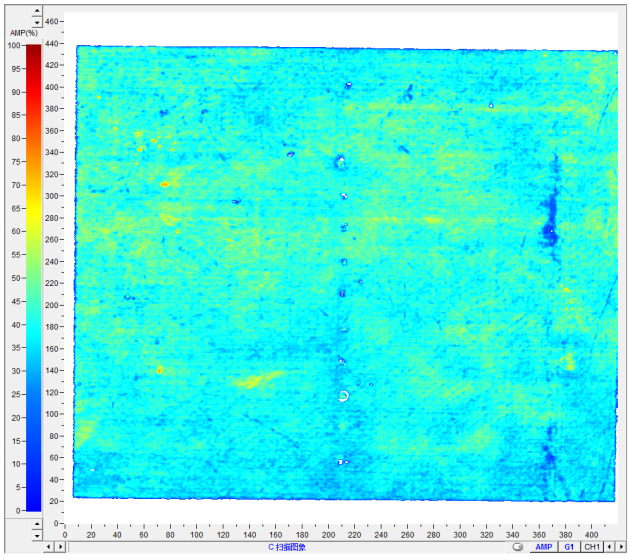

Figure 8: Photograph by C scan

The localization analysis results based on the location algorithm proposed in the 2.2 section, are given in Table 3. It can be seen that the maximum error is 1.88cm and the minimum error is 0.36cm for the specimen. The calculated locations are generally in agreement with the testing impact locations with errors accepted for engineering applications.

We estimate that there are three main factors to cause errors. Firstly, some analytical errors for the amplitude of the impact wave obtained from the signals received by the strain gauges due to the accuracy of the sensors and the noise of the signals. Secondly, the precision of B and α coefficient calculated by the least-squares cure-fitting method is not high enough, resulting in calculation deviation. Further research is ongoing to improve the impact localization scheme developed in this paper to take into account the attenuation model in CFRP composite materials. Finally, there are inevitable errors introduced by the manual excitation with the gas gun in the impact experimental testing due to lack of precision in manual operations.

The regularity of error is not strong, as can be seen in the Table 3. On the whole, the distance from the impact source to the locations of the sensors may potentially influence the precision of the impact localization results. If the impact source is too far away from the sensors, the signals received by the sensors will become weaker due to the dispersion of wave propagation and the signal noise will be higher, which could induce more errors. However, this kind of influence obtained in this study is inconclusive. This may be attributed to the fact that the laboratory testing samples are pretty small and the impact sources are not very close to the edge of the plates.

5 Conclusions

In this paper, the method of the impact reverse localization using energy attenuation is proposed. The strain gauges are attached to the carbon fiber reinforced base laminate, and the impact signal is collected by strain gauges. The attenuation model is fitted by the least-squares curve-fitting method, and the attenuation factor is determined. According to the attenuation model proposed in 2.2 section, the impact point can be reverse localization.

In order to verify the location method in this paper, the specimen of CFRP with symmetrical stacking $[0/45/90/-45]_{2s}$ is chosen. The experimental results show that the mean value of the error ratio is 8.77, which proves that the proposed method can be applied to the low velocity impact positioning of carbon fiber reinforced composite laminates.

Acknowledgement: The technology research project of Jiangxi Provincial Department of Education (No.GJJ180509) and initial fund for Doctors (EA201807238, EA201907279)

References

[1] J.Frieden, J.Cugnoni, J.Botsis,T. Gmür, Low energy impact damage monitoring of composites using dynamic strainsignals from FBG sensors – Part I: Impact detection and localization, Com-

pos.Struct. 94(2012)438-445.
[2] E. Kirkby, R.D.Oliveira, V.Michaud, J.A.Manson, Impact localisation with FBG for a self-healing carbon fibre composite structure, Compos. Struct. 94(2011)8-14.
[3] A.Wagih, P.Maimí, N.Blanco, J.Costa, A quasi-static indentation test to elucidate the sequence of damage events in low velocity impacts on composite laminates, Compos. Part A. 82(2016)180-189.
[4] H.Jeong, Y.S.Jang, Wavelet analysis of plate wave propagation in composite laminates, Compos.Struct. 49(2000) 443-450.
[5] Z.Su, L. Ye, Y.Lu, Guided Lamb waves for identification of damage in composite structures: A review, J. Sound. Vib. 295(2006)753-780.
[6] G.Zhao, H.Hu, S.Li, Localization of impact on composite plates based on integrated wavelet transform and hybrid minimization algorithm[J], Compos. Struct. 176 (2017) 234–243.
[7] I.Trendafilova, R.Palazzetti, A.Zucchelli, Delamination Assessment in Structures Made of Composites Based on General Signal Correlation, Int.J. Struct Stab Dyn. 14(2014)13-26.
[8] M.Johnson, Waveform based clustering and classification of AE transients in composite laminates using principal component analysis, Ndt. E. Int. 35(2002) 367-376.
[9] F.Kerber, H.Sprenger, M.Niethammer, *et al.*, Attenuation analysis of lamb waves using the chirplet transform, Eurasip.J.Adv.Sig.Pr. 1(2010)1-6.
[10] N.Hu, T.Shimomukai, C.Yan, H.Fukunaga, Identification of delamination position in cross-ply laminated composite beams using S0, Lamb mode[J] Compos.Sci.Technol. 68(2008)1548-1554.
[11] A.E.Mahi, M.Assarar, Y.Sefrani, *et al.* Damping analysis of orthotropic composite materials and laminates, Compos. Part B Eng. 39(2008)1069-1076.
[12] A. H.Nayfeh, M.J.Anderson, Wave Propagation in Layered Anisotropic Media with Applications to Composites, J.Acoust.Soc.Am. 108(2000)471-472.
[13] I.Bartoli, A. Marzani, FLD.Scalea, E.Viola, Modeling wave propagation in damped waveguides of arbitrary cross-section, J. Sound. Vib. 295(2006)685–707.
[14] Sohn H, Park G, Wait J R, *et al.* Wavelet-based active sensing for delamination detection in composite structures[J] Smart Materials & Structures, 2003, 13(1):153.
[15] Ip K H, Tse P W, Tam H Y. Extraction of patch-induced Lamb waves using a wavelet transform[J] Smart Materials & Structures, 2004, 13(4):861.
[16] S.Yuan, L. Wang, G. Peng. Neural Network Method Based On A New Damage Signature For Structural Health Monitoring, Thin.Wall.Struct. 43(2005)553-563.
[17] I.M.Daniel, T.Liber, R.H.Labedz, Wave propagation in transversely impacted composite laminates, Exp.Mech. 19(1979)9-16.